Extension of a tuned log spiral of revolution fluorescence XAFS detector, designed for optimal detection of a particular element Z, to XAFS of elements other than Z

D. M. Pease, M. Daniel, J. I. Budnick, B. Taylor, A. Frenkel, K. Pandya, I. K. Grigorieva and A. A. Antonov

Extension of a tuned log spiral of revolution fluorescence XAFS detector, designed for optimal detection of a particular element Z, to XAFS of elements other than Z

D.M. Pease,[a] M. Daniel,[a] J.I. Budnick,[a] B. Taylor [a], A. Frenkel,[b] K. Pandya,[c] I.K. Grigorieva [d], and A.A. Antonov [d]

[a]*Physics Department, University of Connecticut, Storrs, Connecticut,* [b]*Materials Research Laboratory, University of Illinois at Urbana-Champaign, Urbana, Illinois,* [c]*Brookhaven National Laboratory, Upton, New York and* [d]*Optigraph Corporation, Moscow, Russia. E-mail: pease@ims.uconn.edu*

Recently, it has been demonstrated that an x-ray detector in the form of a log spiral of revolution, covered with highly oriented pyrolytic graphite, is an excellent device for obtaining the fluorescence XAFS of an element of interest in the presence of competing fluorescence from other elements. In the present work we investigate the capabilities of a log spiral of revolution (LSR) detector, with a geometry optimized for one element (in this case Cr), if used for XAFS of other elements.

Keywords: Dilute species XAFS, fluorescence XAFS

Introduction

A logarithmic spiral has the defining characteristic that all rays from a focal point meet the spiral at the same angle. It has been long known that the log spiral shape could be used for x-ray applications for which the rays emanating from a focal point strike the log spiral at the correct Bragg angle for a crystal monochromator formed to the log spiral geometry (de Broglie, 1914). The development of a process in Russia whereby highly oriented pyrolytic graphite (HOPG) can be deposited onto smooth surfaces of any shape (Antonov, 1991) therefore makes a log spiral of revolution practical for removal of competing fluorescence or scatter from the desired fluorescence of an atomic species of choice in an XAFS experiment. A logarithmic spiral does not reflect rays to true focus, but concentrates the ray bundle into a small region where the reflected x-rays can be detected by a non energy dispersive detector such as an annular ion chamber or an array of (PIN) diodes. The solid angle obtainable with a log spiral monochromator significantly exceeds that available with Johann bent or Johannson ground and bent focusing (Pease, 2000; Hastings, 1978).

Recently, we have demonstrated that a (LSR) HOPG detector designed for detection of Cr can be used to obtain useful XAFS under circumstances for which conventional ion chamber detectors are unusable because of background fluorescence and in situations for which energy dispersive detectors will exhibit saturation effects (Pease, 2000). We have obtained excellent Cr XAFS for a $V_{.99}Cr_{.01}$ sample using the log spiral detector even though the Cr signal is completely overwhelmed by the V EXAFS when a conventional ion chamber is used. In these experiments, it is important to make use of a "blocking shield" which prevents detection of the fluorescence rays which travel directly from the sample to the PIN diode array. A schematic representation of a half slice through a LSR detector is shown as an insert in Fig. 1.

Two weaknesses of the present LSR detector are that (1) a focused beam is required for optimum performance, and (2) the LSR shape is not tunable to be optimized for more than one energy. Although the HOPG covering process is surprisingly cost effective, so that one could manufacture a series of LSR detectors for different elements, it would be of interest to determine if an LSR detector designed to optimally detect fluorescence from one element can be usefully applied for detection of other atomic species. We have investigated three methods by which this may be accomplished: (1) tuning the sample plane position to maximize the signal from elements of atomic number Z plus or minus one (using an LSR shape optimized for atomic number Z), (2) tuning the LSR to detect the K_β line of the Z-1 element rather than the K_α line of the optimal Z element, (3) using a high order reflection from the HOPG to detect high energy edges.

Experimental Methods and Results

We compare data obtained at two different synchrotron radiation beam lines. For a $Cr_{.15}Ti_{.05}V_{.80}$ alloy of interest for fusion reactor wall applications we use the focused line at the X-16 beam line at the National Synchrotron Light Source (NSLS), with a flux of approximately 1.3×10^{10} photons per second in a 1mm square spot size. We also performed experiments at the unfocused X-11 line at the NSLS. Here we used the smallest spot allowed by the hutch slits, which was 1 mm x 2 mm, and obtained a flux of 1×10^9 photons per second. Data obtained under these conditions was just adequate for concentrated samples, and may not correspond to the best energy resolution of the LSR because of the relatively large spot size.

Fig. 1 below illustrates the performance of the LSR in rejecting the V XAFS from the Cr XAFS for a $Cr_{.50}V_{.50}$ alloy, data obtained by tuning to the Cr K_α line, and comparing this behavior with the rejection of the Ti XAFS from the V XAFS in a $V_{.50}Ti_{.50}$ alloy, data obtained by tuning to the V K_β line. For the $V_{.50} Ti_{.50}$ alloy, one makes use of the fact that the V K_β energy is only 12 eV away from the Cr K_α energy, well within the resolution limit of HOPG for a LSR shape optimized for detection of Cr K_α. The $Cr_{.50}V_{.50}$ comparison data is published in Pease, et. al. and is obtained at the X-11 line at the NSLS. The $Ti_{.50}V_{.50}$ data is obtained at the X-16 focused line at the NSLS. The rejection of V relative to Cr in $Cr_{.50} V_{.50}$ is about a factor of ten relative to the step height ratio obtained using an ion chamber, a limit which is largely determined by the relative intensity of the V K_β relative to the Cr K_α line. The new result of the rejection of Ti relative to V in a $V_{.50}Ti_{.50}$ alloy shows a comparable rejection ratio.

In Fig. 2 we illustrate the use of the LSR to remove diffraction peaks from both Cr and V edges in a $V_{.80}Cr_{.15}Ti_{.05}$ alloy of interest for fusion reactor vessel wall applications (Bloom, 1998). We also illustrate that one can tune the LSR to emphasize or minimize the Mn XAFS   for a $Cr_{.80}Mn_{.20}$ alloy. The negative step at the position of the Mn edge in curve C is due to the removal of photons from the Cr excitation channel at the energy onset of the Mn K edge. No shaft encoder is installed on the present version of the LSR, and the tuning of the sample position resulting in the differences between C and D of Fig. 2 was carried out by hand using trial and error and pencil markings. A rough estimate of the displacement of the sample plane corresponding to curves C versus D is one eighth of an inch.
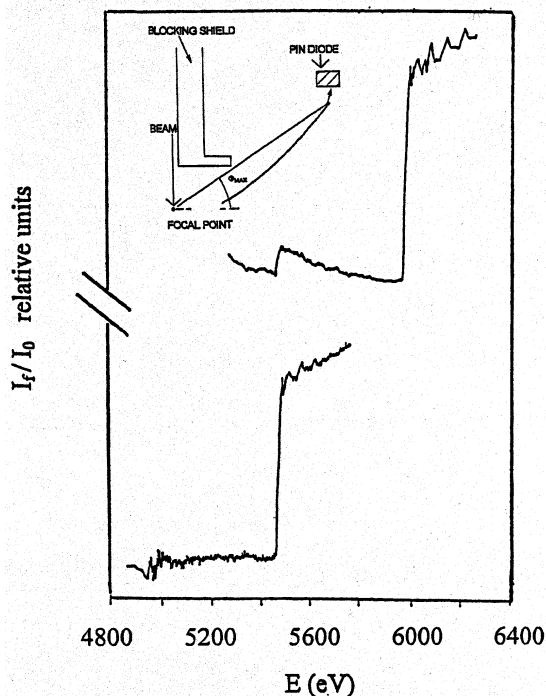
336   *J. Synchrotron Rad.* (2001). **8**, 336–338

Fig. 1   Comparison scans of XAFS for a $Cr_{.50}$ $V_{.50}$ alloy (top), LSR transmitting Cr K_α, and a $Ti_{.50}V_{.50}$ alloy (bottom), LSR transmitting V K_β. The Ti, V, and Cr thresholds are at 4966, 5465, and 5989 eV, respectively. Insert: schematic of LSR.
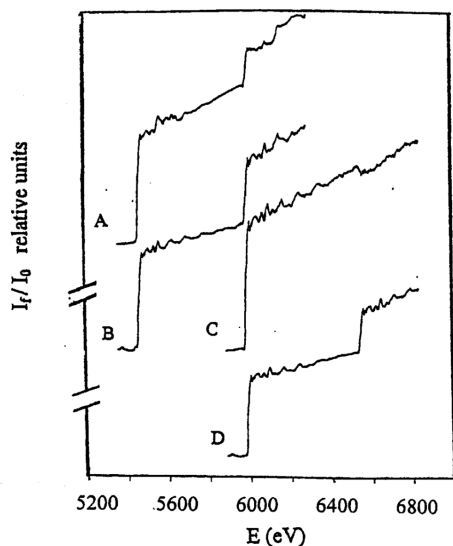

Fig. 2   A, LSR set to transmit both V and Cr edges of a $V_{.80}Cr_{.15}Ti_{.05}$ alloy, blocking shield removed to allow transmission of diffraction peaks; B, same as A but with blocking shield in place to remove diffraction peaks; C, $Cr_{.80}Mn_{.80}$ alloy XAFS, LSR tuned to transmit Cr but reject Mn K_α; D, same as C but with LSR tuned to transmit both Cr and Mn K_α (Pease, 2000).

We have recently performed new exploratory studies investigating the possibility of using our Cr optimized LSR for detecting high energy edges using the high order 004 reflection of HOPG, instead of the most intense 002 reflection used for the

results described above.   We were motivated to perform these experiments by the fact that lead and arsenic are two particularly important elements from the standpoint of environmental pollution of soils (Steinnes, 1989) and furthermore, the energy of the arsenic emission line and the lead $L_{\alpha 1}$ emission line are greater than the energy of the Cr K_α line by factors of 1.95. These experiments were performed at the unfocused X-11 line of the NSLS. It is interesting that the powder diffraction intensity of the 004 graphite reflection, as listed in a published diffraction file, is less than the intensity of the 002 reflection by a factor of 25 (JCPDS powder diffraction file, 1995). However, from experimental studies by Freund, et. al. (1996), the total flux in the 004 reflection for $\lambda/2$ was only less than that in the 002 reflection for λ by about a factor of 3, if λ corresponds to 4 keV photons. The fact that this ratio is only 3, as opposed to the listed ratio of 25 from powder diffraction data at one energy, comes about in part because of the fact that the reflectivity of HOPG increases in going from 4 to 10 keV. Furthermore, air absorption for the higher energy photons is negligible, and germane to our experiment, the L emission fluorescence yield of lead is enhanced over the K emission fluorescence of Cr. However, the thickness of the HOPG in our apparatus may not be adequate for photons corresponding to the lead edge excitation energy. An insufficiently thick HOPG covering would lower the intensity and could have an influence on the resolution.

A simple relationship which can be readily derived between angular spread of Bragg angle $d\theta$ and consequent energy resolution dE is given by the equation:

1. $dE \sim -E (\cot \theta \, d\theta)$

If one lets $d\theta$ represent the angular spread due to HOPG mosaicity, one expects that the resolution in absolute energy will degrade for the higher energy case. Our experiments indicate that the energy resolution of our Cr optimized LSR degrades for the higher energies relative to the Cr K_α line energy by more than can be accounted for by the above equation, since we were unable to discriminate gold relative to lead L edge step heights for test foils of lead versus a gold alloy. The corresponding gold and lead emission lines are separated by 838 eV. In contrast, at lower energies we obtain excellent rejection of Mn versus Cr K_α step heights, and the corresponding emission lines are in this case separated by only 484 eV.

On the other hand, the energy separation between the fluorescence radiation and the scatter in an XAFS experiment also increases for the case of the very high energy edges for which the resolution worsens. Thus, the Cr K_α line is separated from the Cr K edge threshold energy by 574 eV, whereas the lead $L_{\alpha 1}$ line is separated from the lead L_3 absorption threshold by 2.5 keV. We therefore performed experiments in which adjacent lead and Cu foils were placed at the focus of the LSR. We excited first the Cu K edge and second the lead L_3 edge, since the corresponding emission lines are separated by 2.5 keV, the same energy separation as the lead emission relative to incident beam scatter in an experiment in which the lead L_3 edge is excited. We by this means simulate the rejection of scatter relative to lead fluorescence that would result in a hypothetical experiment on dilute lead samples made possible by use of an intense, focused beam source.

Experiments were performed at the X-11 beam line of the NSLS using Si (111) crystals to monochromatize the incident beam. The beam was 1 mm x 2 mm in dimension, and as nearly as we could adjust the samples, 1 mm of the horizontal incident beam spot was

striking the Cu and 1 mm was striking the Pb. By comparing Cu versus lead intensities with and without the blocking shield in place, other conditions being constant, we measured the rejection of Cu relative to lead XAFS step heights due to the LSR. By so doing we compare the acceptance by the LSR of the Cu fluorescence due to the far tail of the 002 reflection profile, versus the acceptance by the LSR of the lead fluorescence due to the peak of the 004 reflection. We obtain a rejection of Cu relative to lead step heights equal to a factor of five. Our XAFS scan for the lead L_3 edge, ten scans averaged, cannot be shown because of space limitations, but is reasonably good data considering the non-ideal conditions of the experiment.

Comparison to Energy Dispersive Detectors

We have recently characterized the intensity and mosaic spread of various thicknesses of the form of HOPG used in our LSR. Films of thickness, in millimeters, of .01, .02, .05, .15, .2, .25, .3, and .4 were deposited on glass slides and compared to good quality bulk HOPG. Rocking curves were obtained, using the Cu K_α emission line, with two different laboratory facilities. In one set up, the incident beam was collimated by a silicon monochromator and the samples were rocked. In another set up, the incident x-ray beam was rendered parallel by a parabolic mutilayer mirror and the detector and source rocked with a stationary sample. These two different, but equivalent experiments yielded comparable results, which are of interest in the present context. The 0.2mm HOPG, corresponding to the thickness used in this LSR, has a mosaic spread close to twice that of the bulk HOPG, which in turn has a mosaic spread of half a degree. The 0.2 mm film has a brightness which is about 60% of the bulk HOPG. On the other hand, .05 mm material has a mosaic spread close to that of bulk material, about .57 degrees, and an intensity half of the bulk HOPG at the Cu K_α line. The brightness of bulk HOPG at this energy is about 50 % (Sparks), and the value of ΔE obtained by inserting a 0.5 degree angular spread in equation 1 is equivalent to 130 eV at the Cr K_α line. The corresponding energy spread for the 0.2 mm HOPG used in our present LSR is about 260 eV for Cr detection. If thinner HOPG were to be used in a future LSR the resolution could improve by a factor of two. The brightness of the HOPG used in our LSR is about 25% at the copper line energy and is expected to be somewhat less than this at Cr because of increased absorption by the HOPG at longer wavelengths. The solid angle of our LSR is 17% of 4π, which could be improved in future models. The main advantage of the LSR is for applications in which a dilute element XAFS is measured in a concentrated matrix of an element to the left of the desired element in the periodic table. At present, the PNC-CAT beam line at the APS is capable of placing an incident beam of $\sim 1\times10^{13}$ photons per second in a spot that is within the acceptance of the LSR. Assuming a fluorescence yield of 20%, air attenuation of 50% , and a solid angle of 17 % of 4π yields an estimated 1.7×10^{11} undesired photons which could be rejected by the LSR, which, unlike energy dispersive detectors, does not saturate.

The performance of multi-element, energy - dispersive detectors varies, and is continually improving. Our own experience with the 13 element detector used at the X-11 line at the NSLS is that at optimum resolution settings this device begins to miss counts if, at the Fe K_α line, the count rate exceeds 20,000 photons per second per channel. The purchase specifications for a more modern multi element detector used at the PNC-CAT line at the APS is that at 5.9 keV an output count rate of 200 kiloherz for input count rate of 300 kiloherz is required at better than 300 eV resolution (D.I Brewe, private communication). A custom made state of the art, monolithic, multipixel Ge detector array used at

Lawrence Berkeley National Laboratory can be operated with resolution ranging from 310 eV at 3.65 keV to 345 eV at 20 keV at 167 kiloherz per channel, or 390 eV at 20 keV at 740 kiloherz per channel. This device utilizes four channels. (N. Madden, L. Fabris, J.J Bucher, D.K. Shuh, and C.H. Booth, private communication). It would seem that at present, the very best that can be done with multi-element energy dispersive arrays would be $\sim$ 10 channels at a million counts per second per channel, at about 300 eV resolution for energies in the vicinity of the Cr $K\bullet$ line. In sum, the present LSR has comparable resolution to energy dispersive arrays, with a possibility of significant future improvement of the LSR in this regard. The ability of the LSR to reject unwanted photons without saturation at third generation sources ($\sim10^{11}$ photons per second) is much improved over the saturation limit of even the best energy dispersive arrays ($\sim10^7$ photons per second). This enhancement should result in improved detection capabilities for the LSR even given 10% brightness of the HOPG. However, it would be most interesting to use the LSR *together* with a multi-element energy dispersive array. Then the LSR would reject the unwanted photons which degrade the performance of the energy dispersive array, and one could multiply the resolutions of both instruments.

References

Antonov, A.A. , Baryshev, V.B., Grigorieva, I.G., Kulipanov, G.N., & N.N. Shcipkov, (1991) *Nuclear Instruments and Methods in Physics Research* **A308.**

Bloom, E.(1998), *Journal Nuclear Materials* , 258 - 263.

DeBroglie, M.& Lindemann, F.A. (1914). *Compt. Rend* **158**, 944

Freund, A., Munkholm, A, & Brennan, S.(1996), *SPIE* **Vol. 2856**, 68 - 86.

Hastings, J.B., Perlman, M.J., Oversluizen, P., Eisenberger, P., & Brown, J.(1978) *5th annual SSRL Users Group Meeting, 1978, SSRL Rept. No. 78 - 09.*

JCPDS powder diffraction file 1995; PDF-2 data base set 41, *International Centre for Diffraction Data*, Newtown Square, Pennsylvania

Pease, D.M. Daniel, M., Budnick, J.I.,Rhodes, T.,Hammes, M., Potrepka, D.M., Sills, K., Nelson, C., Heald, S.M., Brewe, D.I., Frenkel, A., Grigorieva, I.A., & Antonov, A.A.(2000), *Rev. Sci. Instr* **78**, 3267 - 3273.

Sparks, C.J., Metals and Ceramics Division, Oak Ridge National Laboratory, Annual Progress Report, ORNL-3970, 1966, 57.

Steinnes, E., Solberg, W., Petersen, H.M., and Wren, D.M.(1989), *Water, Air, and Soil Pollution*, **45**, 207-208.